JOURNAL OF SOLID STATE CHEMISTRY 26, 281–291 (1978)

Vibrational Spectra of Alkali Hydrogen Selenites Selenous Acid, and Their Deuterated Analogs*

C. A. CODY† AND R. C. LEVITT

Department of Chemistry and Center for Materials Research, University of Maryland, College Park, Maryland 20742

AND RAMPUR S. VISWANATH AND PHILIP J. MILLER

Department of Chemistry, University of Detroit, Detroit, Michigan 48221

Received December 23, 1977; in revised form April 17, 1978

The infrared and Raman spectra of alkali hydrogen selenites [(MHSeO$_3$), where M = Li, Na, K, or Cs], selenous acid (H_2SeO_3), and their deuterated analogs have been recorded and interpreted. The internal mode frequencies observed in sodium hydrogen selenite, selenous acid, and sodium trihydrogen selenite are used to generate general valence force constants for $HSeO_3^-$ and H_2SeO_3 under the assumption of C_s geometry for each species. Calculations of observed deuterium frequency shifts are made to aid in the assignments of the various internal modes. A low-temperature proton-triggered phase transition is observed in CsHSeO$_3$ and is confirmed in KHSeO$_3$. A discussion of the effects of proton order and disorder upon the selenite frequencies is also presented.

Introduction

During our infrared and Raman investigation of the alkali trihydrogen selenites [MH$_3$(SeO$_3$)$_2$] and associated phase transitions, it became necessary to reinvestigate the vibrational spectra of SeO_3^{2-}, $HSeO_3^-$, and H_2SeO_3. Even though examination of the literature revealed numerous vibrational studies of these ions (*1–5*) several problems would be evident if one attempted to use these results to interpret the spectra of the alkali trihydrogen selenites. For instance, Walrafein (*4*) studied these ions in aqueous solutions, and thus no generalization about the effect of the various crystal splittings could be made. Torrie (*2*) examined sodium hydrogen selenite and selenous acid, but his assignments and those of Khanna *et al.* (*1*) were in conflict. In an attempt to clarify the situation, we have recorded the infrared and Raman spectra of polycrystalline lithium, sodium, potassium, and cesium hydrogen selenite, selenous acid, and their deuterated analogs. Low-temperature Raman studies were carried out to detect possible transitions, and a more general valence force field calculation than any previously attempted was also carried out to clarify the assignments.

In addition to the results of the above study, we also present an interpretation of the effects of proton order and disorder upon the vibrational frequencies of selenite (SeO_3^{2-}) units. Brief references are made to some of our spectroscopic studies of the order–disorder phase transitions in the alkali trihydrogen selenites [MH$_3$(SeO$_3$)$_2$].

* This work was supported by a research grant from the Center of Materials Research, University of Maryland, College Park, Md. 20742.

† Present address: NL Industries, Hightstown, N.J. 08520.

0022–4596/78/0263–0281$02.00/0

Experimental

Single crystals of each alkali hydrogen selenite ($MHSeO_3$) (where M = Li, Na, K, or Cs) were grown by slow evaporation of an aqueous solution formed by dissolving 2 moles of SeO_2 and 1 mole of M_2CO_3 into distilled water. Single crystals of selenous acid, H_2SeO_3, were grown by dissolving SeO_2 into distilled water and allowing the solution to evaporate. Well-formed crystals of each compound were grown in several days. Deuterated crystals of each material were grown by dissolving well-formed crystals of each salt into 99.8% D_2O and evaporating to dryness in an N_2 atmosphere.

For the Raman studies large transparent crystals of each material were ground into a fine powder and then pressed into a small pellet. The Raman spectra were obtained using a Jarrell–Ash double monochromator equipped with a Carson Model Argon ion laser (total power, 5 W). The exciting line was 5145 A. Spectra were obtained with ca. 1 W of power and with resolution set at ~3 cm^{-1}. Low-temperature spectra were recorded at 77°K using a conventional liquid nitrogen Dewer sample container. Infrared spectra were obtained via the standard KBr wafer technique. Infrared spectra were recorded on a Digilab FTS-14 spectrophotometer over the region 4000 to 400 cm^{-1} with resolution set equal to 4 cm^{-1}. All spectra were ratio plotted; 100 scans of the sample pellet versus 100 scans of the blank reference beam were ratioed and plotted as a transmission spectra. Infrared spectral plots displayed in this article were scale expanded by the FTS-14 (i.e., the lowest transmission value was set at 0% and the highest transmission value was set at 100%) and were then plotted. Periodically, the calibration of the FTS-14 was checked with a polyethylene film.

Discussion and Results

Only a limited number of investigations have been reported on the alkali hydrogen selenites and selenous acid. Torrie (*2*) recorded infrared and Raman spectra of $NaHSeO_3$ and H_2SeO_3, as did Simon and Paetzold (*3*), who also included $KHSeO_3$ in their study. Vedam and Pepinsky (*7*) optically observed a phase transition in $KHSeO_3$ at −39°C; the lack of a sizable dielective anomoly indicated that the low-temperature phase was nonferroelectric. No pertinent studies of $LiHSeO_3$ or $CsHSeO_3$ are reported in the literature.

Selenous acid has been examined by X-ray and neutron diffraction (*8*). The crystal structure is reported to be $P_{2_1?2_1?2_1}$ with $Z = 4$ and features hydrogen bonds of 2.667 and 2.621-Å lengths. Protons residing within both hydrogen bonds appear to be well ordered, i.e., to occupy single-minimum-type potential wells. Selenous acid contains a bifurcated hydrogen bond, a feature not found in any of the alkali trihydrogen selenites (*6*).

The room-temperature Raman spectra of H_2SeO_3, $NaHSeO_3$, $LiHSeO_3$, and $LiDSeO_3$ are shown in Fig. 1. The Raman spectra of $KHSeO_3$ and $CsHSeO_3$, at room temperature and at liquid nitrogen temperature, are shown in Fig. 2. The infrared spectra of all four alkali hydrogen selenites, recorded at room temperature are illustrated in Fig. 3. The frequencies observed in the internal mode region for each crystal are presented in Tables I and II.

The differences between the respective Raman and infrared sets of spectra arise primarily from the facts that the Li^+ and Na^+ salts contain ordered protons (spectra are characteristic of $HSeO_3^-$ units), while the K^+ and Cs^+ salts contains disordered protons (spectra are characteristic of SeO_3^{2-} units). The spectrum of selenous acid is characteristic of H_2SeO_3, confirming the neutron diffraction suggestion that this crystal contains only ordered protons at room temperature.

The distinction of whether or not a given hydrogen-bonded crystal contains ordered or disordered protons can be based upon the frequencies and breadths of the internal modes. These conditions were used to establish the conclusions presented above; a lengthy dis-

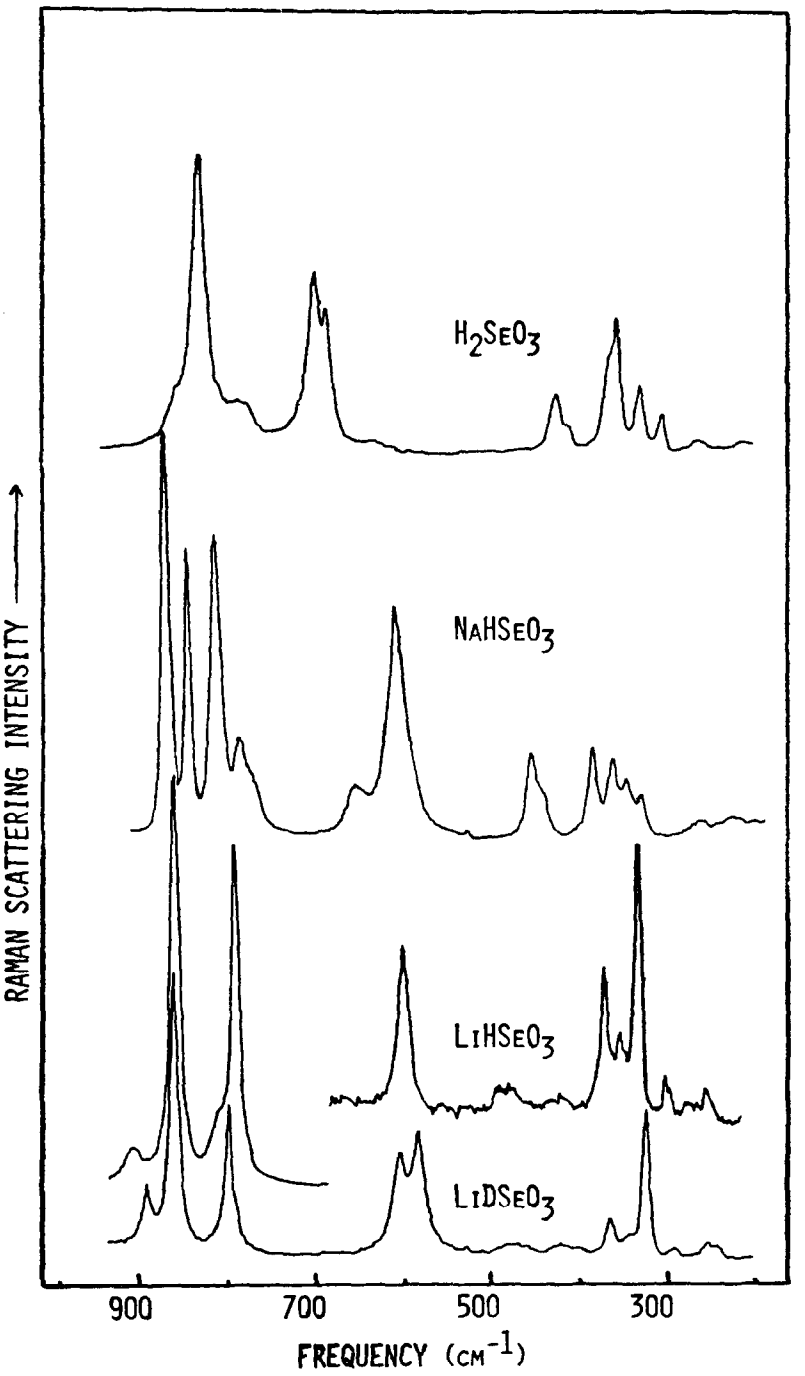

FIG. 1. The room-temperature Raman spectra of polycrystalline $LiHSeO_3$, $NaHSeO_3$, $LiDSeO_3$, and H_2SeO_3.

cussion of these conditions and their effects upon the selenite frequencies is given in the next section.

The Raman spectra of the K^+ and Cs^+ salts recorded at liquid nitrogen temperatures (spectra are included in Fig. 2) indicate that

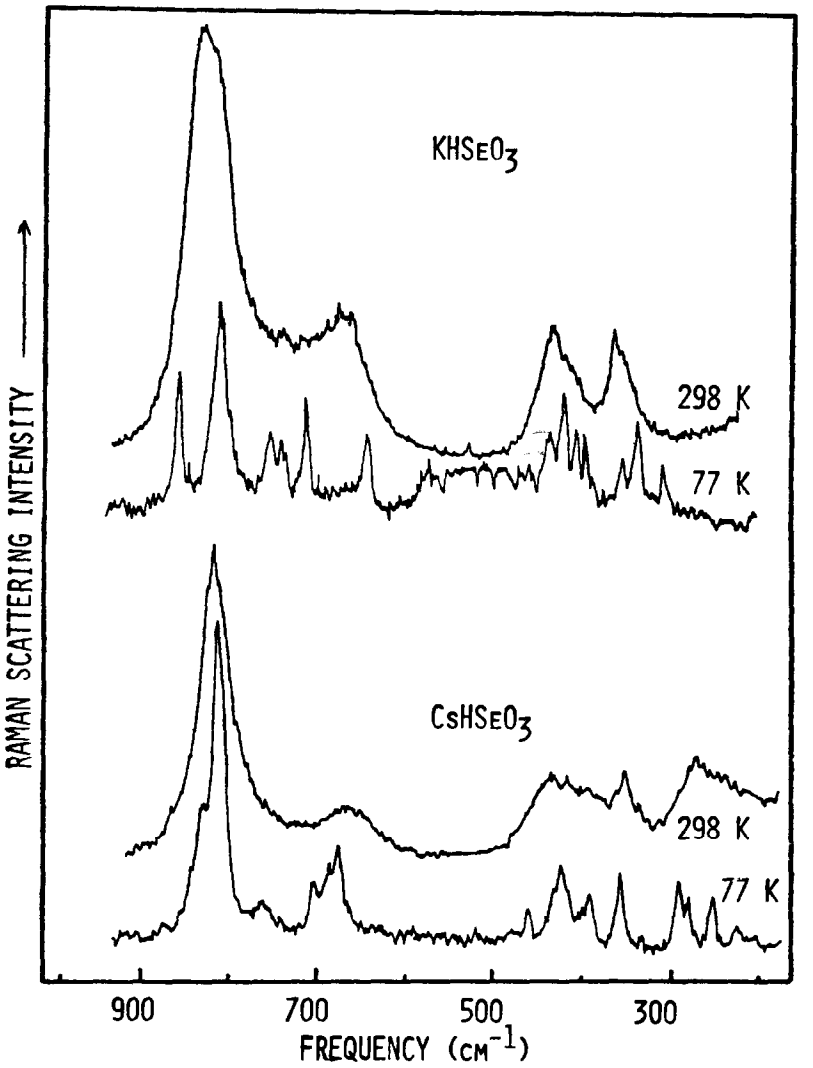

FIG. 2. The Raman spectra of polycrystalline $KHSeO_3$ and $CsHSeO_3$ at room temperature and liquid nitrogen temperature.

both of these compounds go through an apparent phase transition to ordered states. Spectra of the K^+ and Cs^+ salts at liquid nitrogen temperatures have the appearance of the $HSeO_3^-$ ion, in the internal mode region, indicating that these transitions are due to the ordering of protons. This conclusion is based upon the extreme narrowing of the bandwidths, the appearance of $HSeO_3^-$ frequencies, and the disappearance of the SeO_3^{2-} frequencies at liquid nitrogen temperature. The low-temperature spectra of the K^+ and Cs^+ salts resemble the room-temperature spectra of the proton-ordered Na^+ and Li^+ salts. These spectroscopic arguments have been used by others to detect phase transitions in the KDP-type crystals (*9*, *10*).

The major spectral differences in the five crystals, at low temperatures, can be attributed to differences in each lattice geometry, crystal field effects, and varying hydrogen bond parameters. Because of the lack of structure

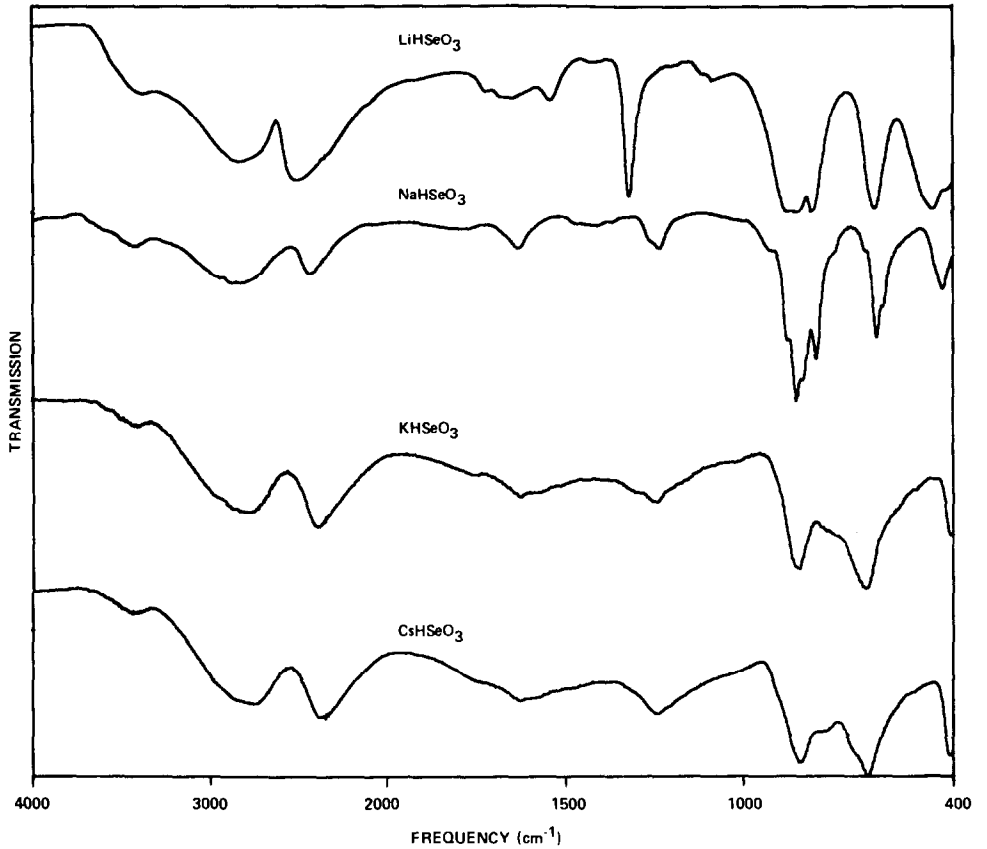

FIG. 3. The room-temperature infrared spectra of polycrystalline alkali hydrogen selenites.

information, however, no correlations of frequencies and intensities versus molecular parameters can be made at this time, although from the large number of peaks observed and the lack of coincidences in Table I, it is apparent that each crystal contains several species in the unit cell.

It is interesting to note that the hydrogen bond stretching regions (3600–1400 cm^{-1}; Fig. 3) of all the alkali hydrogen selenites, trihydrogen selenites (*6*), and selenous acid are very similar; yet major differences in molecular parameters are evident from the internal mode frequencies. Even the presence of a bifurcated hydrogen bond in selenous acid does not appreciably perturb the O–H stretching region, indicating that intrabond proton dynamics are not the controlling factors in crystals of these types.

The low-temperature results have confirmed the optical detection of a phase transition in $KHSeO_3$ and have discovered a previously unreported phase transition in $CsHSeO_3$.

General Valence Force Field Calculations

The spectroscopic detection of protons residing in single-minimum or double-minimum potential wells (static or tunneling protons), and the relationship between proton behavior and ferroelectric activity in crystals such as $LiH_3(SeO_3)_2$, $NaH_3(SeO_3)_2$, and KH_2PO_4 can be based upon the breadth, number, and frequency of internal modes seen in the vibrational spectrum for each phase of a compound. Any of the alkali hydrogen or trihydrogen selenites can be considered to be built up from a network of cations and SeO_3^{2-}

TABLE I

OBSERVED INTERNAL MODE FREQUENCIES OF $LiHSeO_3$, $NaHSeO_3$, AND H_2SeO_3 (AT ROOM TEMPERATURE)

	$LiHSeO_3$		$NaHSeO_3$		H_2SeO_3	
Assignments[a]	ir	Raman	ir	Raman	ir	Raman
ν_3'	870	867(863)[b]	870 sh[c]	871(871)		
	845		842	845(847)	700	700(686)
ν_3''	800	798(801)	825 sh	813(812)	680 sh	
			788	785(787)	667	689(675)
ν_1	620	602(584)	650 sh	601(587)	865	
			615	583	820 sh	832(832)
			600			
ν_2	455(?)			449(448)		
	420	408(408)	420	439(437)		426(408)
ν_4''		359(359)		378(382)		
				353(355)		332(327)
ν_4'				337(338)		
		320(316)		319(324)		359(349)

[a] See text.

[b] Deuterated species in parentheses.

[c] sh = shoulder.

ions; the SeO_3^{2-} ions are hydrogen bonded together via a proton network. Protons occupying the hydrogen bonds can be static (located in a well-defined position) or rapidly tunneling between minima in some type of intrabond double-minimum potential well. These two different proton environments produce detectable differences in the SeO_3^{2-} ion internal mode frequencies (see Figs 2 and 3). The change from a rapidly tunneling proton to one which is static is believed to drive the phase transition in KDP-type crystals.

Consider, for example, the situation in which protons are intrabond tunneling with a frequency greater than the highest internal mode frequency of the SeO_3^{2-} ion (ν_1 motion). Then, the SeO_3^{2-} ion will see only a time-"averaged" position of the proton. This time-averaged position will be near or at the center of the hydrogen bond, so that the protons can be considered to be equally shared between SeO_3^{2-} ions (denoted as $*SeO_3^{2-}$; the analogous situation with deuterons is denoted as $**SeO_3^{2-}$ in this article).

One of the more pronounced effects of these tunneling protons upon the $*SeO_3^{2-}$ ion is to broaden each $*SeO_3^{2-}$ band in the spectrum markedly. This result is due to the coupling of the vibrational modes of several $*SeO_3^{2-}$ ions, the interaction producing a distribution of frequencies for each mode, i.e., a liquid-like environment. The coupling arises because the proton moves in response to the $*SeO_3^{2-}$ motion and thus transfers the motion to its hydrogen-bonded $*SeO_3^{2-}$ neighbors. As a consequence, broad $*SeO_3^{2-}$ bands observed in any phase of the selenite salts or selenous acid are immediate indications of rapid intrabond proton tunneling.

If tunneling stops, the proton becomes bonded to a particular $*SeO_3^{2-}$ ion. The attachment of the proton to the $*SeO_3^{2-}$ changes the bonding characteristics of this ion, resulting in the new ionic species $H–O–SeO_2^-(HSeO_3^-)$, and consequently, perturbs the vibrational frequencies. The $HSeO_3^-$ bands become quite sharp in the ordered phase because the static proton cannot efficiently

TABLE II

OBSERVED INTERNAL MODE FREQUENCIES OF $KHSeO_3$ AND $CsHSeO_3$

	$KHSeO_3$		$CsHSeO_3$	
Assignments[a]	ir	Raman	ir	Raman
Room temperature				
ν_3	650	665	660 sh[b]	
			645	658
ν_1	835	826	834	816
ν_2	408	423	408	418
		403 sh		385 sh
ν_4		351		333
		341 sh		
Liquid N_2 temperature				
ν_3'		859		824
		813		890
ν_3''		755		745
		743		733
ν_1				692
		716		676 sh
		647		666
ν_2		439		
		424		441
		411		412
		401		401
ν_4''		356		374
		342		366
ν_4'		310		333

[a] See text.

[b] sh = shoulder.

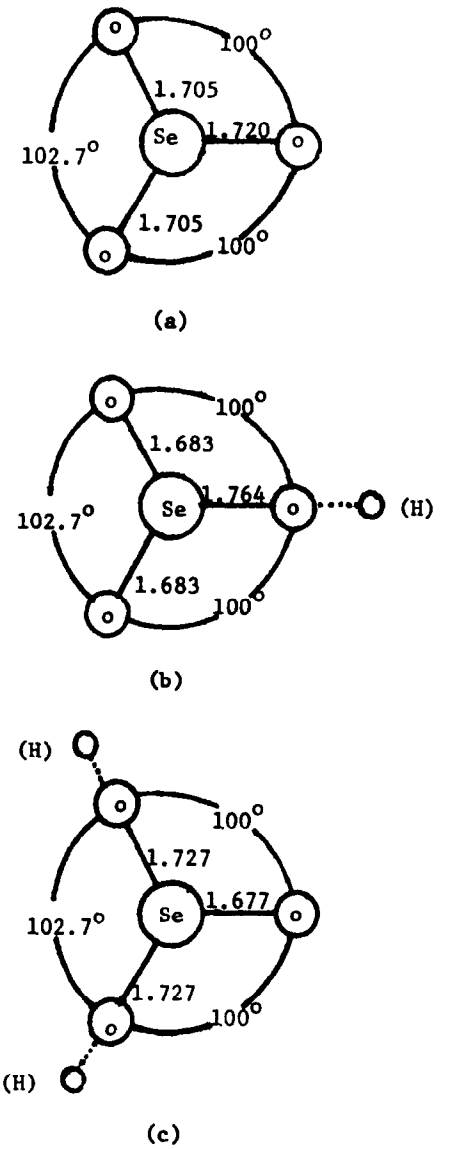

FIG. 4. Bond lengths and angles used in the force constant calculation for (a) SeO_3^{2-}, (b) $HSeO_3^-$, and (c) H_2SeO_3.

couple the $HSeO_3^-$ molecules throughout the lattice.

The bonding of a proton to a $^*SeO_3^{2-}$ ion alters the original frequencies. The formation of an O(1)–H bond within an SeO_3^{2-} ion weakens the corresponding Se–O(1) bond and strengthens the Se–O(2) and Se–O(3) bonds which are not directly bonded to hydrogens. Furthermore, it is not inappropriate to consider the effective mass of O(1) (the designations of the oxygen atoms are described in Fig. 4) to become 17 amu as the proton bonds to O(1), while the effective masses of O(2) and O(3) become 16 amu, respectively, as protons are lost to opposing oxygens of these hydrogen bonds. This mass assumption will also allow comparisons to previous force field calculations carried out by Khanna *et al.* (*1*) and Torrie (*2*).

The changing bond strengths (or force constants) and effective oxygen masses greatly

alter the $*SeO_3^{2-}$ frequencies, the new frequencies being characteristic of $HSeO_3^-$. The presence of $HSeO_3^-$ bands in the spectrum can be used as an indication that one proton has ordered in the crystal lattice.

The hydrogen bond structure of selenous acid (or any of the alkali trihydrogen selenites) is such that ordering of two protons can also produce H_2SeO_3 molecules. The addition of two protons to the $*SeO_3^{2-}$ ion produces changes similar to those mentioned above for $HSeO_3^-$, but different frequencies are expected. Thus, the ordering of two protons in any phase can be rapidly confirmed by the presence of H_2SeO_3 frequencies in the infrared and Raman spectra.

Khanna *et al.* (*1*) carried out a force constant calculation using a generalized valence force field, based upon C_{3v} geometry, to determine the effect of proton tunneling upon the $*SeO_3^{2-}$, $HSeO_3^-$, and H_2SeO_3 frequencies. They carried out their calculations of $HSeO_3^-$ and H_2SeO_3 frequencies by obtaining the force constants of $*SeO_3^{2-}$ (the frequencies having been obtained from the infrared spectra of crystalline Na_2SeO_3); then each of the Se–O bonds that had gained a proton had its stretching force constants weakened by 10%, while each of the Se–O bonds that had lost a proton had its force constants strengthened by 10%. These new stretching force constants were used to calculate $HSeO_3^-$ and H_2SeO_3 frequencies without corresponding changes in bending force constants. Torrie (*2*) repeated the calculation, verified the frequencies, and suggested the possibility of an incorrect assignment—the interchange of ν_1 and ν_3' for $HSeO_3^-$ in Table III. To investigate the possibility of an incorrect assignment, a generalized valence force field calculation (GVF) based upon C_s geometry was undertaken.

The F and G matrices used were those of Cotton and Horrocks (*11*). Under the most general calculation of frequencies for a four-atom molecule having C_s geometry, there are 13 unique force constants. Only 6 force constants were retained in this calculation because only six vibrational frequencies are allowed for a nonlinear four-atom molecule. Following the designations of Cotton and Horrocks (*11*), K_1 represents the Se–O(1) stretching force constants, K_2 the Se–O(2) and Se–O(3) stretching force constants, and K_{12} and K_{22} the stretch interaction constants. The O(1)–Se–O(2 or 3) bending force constant is labeled K_α, the O(2)–Se–O(3) bending force constant is labeled K_β and the bend–bend interaction force constants are labeled $K_{\alpha\beta}$ and $K_{\alpha\alpha'}$.

Actually, interaction force constants like K_{22} and $K_{\alpha\alpha}$ are expected to be different from K_{12} or $K_{\alpha\beta}$, respectively. However, it was felt that the respective pairs would be similar in magnitude and could be easily incorporated into the framework of a six-force-constant calculation simply by defining $K_{12} \equiv K_{22}$ and $K_{\alpha\beta} \equiv K_{\alpha\alpha'}$. In Tables III–VI, the designations

TABLE III

THE STRETCHING FREQUENCIES (cm^{-1}) OF $*SeO_3^{2-}$, $HSeO_3^-$, AND H_2SeO_3 AS COMPUTED BY KHANNA[a] AND TORRIE[b]

C_{3v}	C_s		$*SeO_3^{2-}$	(C_{3v})	$HSeO_3^-$	(C_s)	H_2SeO_3	(C_s)
ν_1	ν_1	Se–O(1) stretch	825[a]	825[b]	651[a]	840[b]	824[a]	820[b]
	ν_3'	Se–O(2,3) symmetric stretch			845	665	683	690
ν_3		Se–O(2,3) degenerate stretch	689	680				
	ν_3''	Se–O(2,3) asymmetric stretch			737	725	624	635

[a] Reference (*1*).
[b] Reference (*2*).

TABLE IV

THE CALCULATED FORCE CONSTANTS OF $*SeO_3^{2-}$

		$*SeO_3^{2-}$ frequencies	Force constant (10^5 dyn/cm)
$\nu_1(A')$	Se–O(1) sym. stretch	800	$K_1 = 5.02$
$\nu_2(A')$	O(2)–Se–O(3) sym. bend	450	$K_\beta = 0.76$
$\nu_3'(A')$	Se–O(2,3) sym. stretch	670	$K_2 = 3.50$
$\nu_3''(A'')$	Se–O(2,3) asym. stretch	660	$K_{22} = 0.18$
$\nu_4'(A')$	Se–O(1,2,3) sym. deformation	335	$K_\alpha = 0.48$
$\nu_4''(a'')$	Se–O(1,2,3) asym. deformation	375	$K_{\alpha\alpha} = -0.02$

K_{22} and $K_{\alpha\alpha}$ are used to denote this procedure. All stretch–bend interaction force constants were set equal to zero because the stretching and bending frequencies are well separated.

The relevant bond lengths and angles used in the calculations of $*SeO_3^{2-}$ force constants are displayed in Fig. 4a. The calculated force constants based upon the observed $*SeO_3^{2-}$ frequencies found in the totally disordered phase of $NaH_3(SeO_3)_2$ are listed in Table IV (*6*). The designations ν_3', ν_3'' and ν_4', ν_4'' result from the correlation of C_{3v} to C_s symmetry. The calculation was performed with $\nu_3' = 670$ cm^{-1} and $\nu_3'' = 660$ cm^{-1} when in fact these modes were observed to be degenerate. This was done to establish general trends in force constants and not to obtain highly accurate force constants.

As tunneling stops, the proton becomes bonded to a particular oxygen of the $*SeO_3^{2-}$ molecule producing $HSeO_3^-$ ($H{-}OSeO_2^-$). The Se–O(1) bond is weakened and the O(1) mass increases to 17 amu, which drives ν_1 to a lower frequency. The remaining Se–O(2, 3) stretching force constants are expected to increase, which in turn drives ν_3' and ν_3'' up in frequency.

The frequencies of $LiHSeO_3$ were used to illustrate this effect and to determine the magnitudes of the expected frequency shifts. The force constants of $HSeO_3^-$ as obtained from the $LiHSeO_3$ frequencies are listed in Table V. The geometry used in the calculation is given in Fig. 4b.

The assignment of the Se–O(1)–H stretching motion, ν_1 at 602 cm^{-1}, follows from the weakening of the Se–O(1) bond upon addition of a proton. K_1 drops from 5.02×10^5 to 3.20×10^5 dyn/cm. This in turn causes the Se–O(2, 3) bonds to strengthen and drives ν_3' and ν_3'' to

TABLE V

THE FORCE CONSTANTS OF $HSeO_3^-$ (FROM $LiHSeO_3$) AND CALCULATED AND OBSERVED $DSeO_3^-$ FREQUENCIES (cm^{-1})

		$HSeO_3^-$ frequencies	Force constant (10^5 dyne/cm)	$DSeO_3$ frequencies	
				Calculated	Observed
$\nu_1(A')$	Se–O(1)–H sym. stretch	602	$K_1 = 3.20$	594	584
$\nu_2(A')$	O(2)–Se–O(3) sym. bend	408	$K_\beta = 0.62$	408	408
$\nu_3'(A')$	Se–O(2,3) sym. stretch	867	$K_2 = 5.42$	866	863
$\nu_3''(A'')$	Se–O(2,3) asym. stretch	798	$K_{22} = 0.58$	798	801
$\nu_4'(A')$	Se–O(1,2,3) sym. deformation	320	$K_\alpha = 0.44$	317	316
$\nu_4''(A'')$	Se–O(1,2,3) asym. deformation	359	$K_{\alpha\alpha} = -0.02$	358	359

TABLE VI

THE EFFECT OF VARYING K_1 AND K_2 UPON THE $HSeO_3^-$ STRETCHING FREQUENCIES

Force constant (10^5 dyn/cm)			Frequencies		
K_1	K_2	K_{22}	$\nu_1(A')$	$\nu_3'(A')$	$\nu_3''(A'')$
5.0	3.5	0.2	800	670	660
4.8	3.9	0.2	761	709	689
4.4	4.3	0.2	730	743	737
4.0	4.7	0.2	695	775	771
3.20[a]	5.42[a]	0.58[a]	602	867	798

[a] Final values from Table V.

867 and 798 cm^{-1}, respectively. As a direct consequence, K_2 increases from 3.50×10^5 to 5.42×10^5 dyn/cm.

Mielke and Ratajczak (*12*) have observed this effect in the H–O–SO_3^- ion (HSO_4^-). Their stretching force constant was 3.98×10^5 dyn/cm for the S–O bond, leaving an attached proton, and 7.26×10^5 dyn/cm for the S–O bonds not having protons directly attached to the oxygens. They assigned the S–O–H stretching motion at 880 cm^{-1} and the remaining S–O stretching motions at 1193, 1156, and 1042 cm^{-1} (*12*).

The observed deuteration frequencies and the results of the calculated frequency shifts support the assignment of ν_1 as an Se–O(1)–H stretch. As the O(1) oxygen mass increases from 17 to 18 amu, ν_1 drops in frequency (observed, 584 cm^{-1}; calculated, 594 cm^{-1}), as expected, but ν_3' and ν_3'' remain insensitive to the mass change, as they should.

Perhaps the most convincing evidence in support of ν_1 as an Se–O(1)–H stretching motion comes from varying K_1 and K_2 over their respective ranges, as seen in Tables IV and V. Decreasing K_1 leads to a decrease in frequency of the 800-cm^{-1} mode; increasing K_2 leads to an increase in the frequency of the 670- and 660-cm^{-1} modes. The results are presented in Table VI and are in good agreement with the earlier assignments and calculation carried out by Khanna *et al.* (*1*).

The force constants of H_2SeO_3 were calculated on the basis of the H_2SeO_3 frequencies reported in Table I. The observed frequencies and calculated force constants are given in Table VII. The geometry used in the calculation can be found in Fig. 4c.

TABLE VII

THE FORCE CONSTANTS OF H_2SeO_3 AND CALCULATED AND OBSERVED D_2SeO_3 FREQUENCIES (cm^{-1})

		H_2SeO_3 frequencies	Force constant (10^5 dyn/cm)	D_2SeO_3 frequencies	
				Calculated	Observed
$\nu_1(A')$	Se–O(1) sym. stretch	832	$K_1 = 5.44$	832	832
$\nu_2(A')$	O(2)–Se–O(3) sym. bend	426	$K_\beta = 0.71$	412	408
$\nu_3'(A')$	Se–O(2,3) sym. stretch	700	$K_2 = 3.99$	685	686
$\nu_3''(A'')$	Se–O(2,3) asym. stretch	689	$K_{22} = 0.22$	672	675
$\nu_4'(A')$	Se–O(1,2,3) sym. deformation	353	$K_\alpha = 0.46$	353	349
$\nu_4''(A'')$	Se–O(1,2,3) asym. deformation	332	$K_{\alpha\alpha} = -0.002$	329	327

The previous calculations and assignments on the $HSeO_3^-$ and $DSeO_3^-$ ions, which were presented in Table V, are further supported by the results of the study on H_2SeO_3 and D_2SeO_3. The ν_3' and ν_3'' modes of H_2SeO_3 are seen to be sensitive to deuterium substitution, both shifting toward lower frequencies by 14 cm^{-1}, whereas ν_1 of H_2SeO_3 is insensitive to deuterium substitution. The consistency between the two sets of calculation supports the assignments.

Conclusion

The calculations were carried out to aid in interpreting and assigning the infrared and Raman spectra of the alkali trihydrogen selenites. The calculation provides useful qualitative information, although absolute quantitative agreement between calculated and observed frequencies is not to be expected in view of the number and nature of the approximations that were made. Also, the hydrogen bond lengths vary from crystal to crystal, which in turn will alter the internal mode frequencies of $*SeO_3^{2-}$, $HSeO_3^-$, and H_2SeO_3 from those reported here. Furthermore, it is well known that the O...O distances change slightly, as do the Se–O distances, upon deuteration; these effects were not included in the calculated frequencies and force constants. The qualitative results of this study, however, do indicate that all protons in $LiHSeO_3$, $NaHSeO_3$, and selenous acid crystals are well ordered, i.e., occupy single-minimum-type hydrogen bonds at room temperature. Furthermore, the $KHSeO_3$ and $CsHSeO_3$ crystals at room temperature contain disordered protons. At liquid nitrogen temperature the K^+ and Cs^+ salts have ordered protons, indicating that both crystals have undergone proton-triggered phase transitions.

The hydrogen bond stretching region of all crystals (1500–3500 cm^{-1}) is very similar to that reported for the alkali dihydrogen phosphates and the alkali trihydrogen selenites. The authors have previously discussed the extreme similarity of this region for KDP-type crystals, their arguments based upon a proton diffusion mechanism controlling the shape, frequency, and number of components seen. A more lengthy discussion can be found in other publications from this laboratory (*6*, *13*).

References

1. R. K. KHANNA, J. C. DECIUS, AND E. R. LIPPINCOTT, *J. Chem. Phys.* **43**, 2974 (1965).
2. B. H. TORRIE, *Canad. J. Phys.* **51**, 610 (1973).
3. A. SIMON AND R. PAETZOLD, *Z. Anorg. Allg. Chem.* **301**, 245 (1959).
4. G. E. WALRAFEIN, *J. Chem. Phys.* **36**, 90 (1962).
5. M. FALK AND P. A. GIGUERRE, *Canad. J. Chem.* **36**, 1680 (1958).
6. C. A. CODY, Ph.D. dissertation, University of Maryland, 1976.
7. R. PEPINSKY AND K. VEDAM, *Phys. Rev.* **114**, 1217 (1959).
8. R. K. LARSEN, M. S. LEHMANN, AND I. SOTAFTE, *Acta Chem. Scand.* **25**, 5 (1971).
9. E. WEINER (AVNEAR), S. LEVIN, AND I. PELAH, *J. Chem. Phys.* **52**, 2881 (1970).
10. Y. SATO, *J. Chem. Phys.* **53**, 887 (1970).
11. F. A. COTTON AND W. D. HORROCKS, *Spectrochim. Acta* **16**, 358 (1960).
12. Z. MIELKE AND H. RATAJCZAK, *J. Mol. Struct.* **18**, 493 (1973).
13. C. A. CODY AND R. K. KHANNA, *Ferroelectrics* **9**, 251 (1975).